Available online at www.sciencedirect.com
SCIENCE DIRECT®
ELSEVIER
Journal of Sound and Vibration 277 (2004) 205–222
JOURNAL OF SOUND AND VIBRATION
www.elsevier.com/locate/jsvi

Vibration analysis of twisted plates using first order shear deformation theory

X.X. Hu[a,*], T. Sakiyama[b], Y. Xiong[b], H. Matsuda[b], C. Morita[b]

[a] *College of Mechanical Engineering, Zhejiang University of Technology, No. 6 District, Zhaohui Xincun, Hangzhou, Zhejiang 310032, China*

[b] *Department of Structural Engineering, Faculty of Engineering, Nagasaki University, 1-14 Bunkyomachi, Nagasaki 852-8521, Japan*

Received 29 November 2002; accepted 27 August 2003

Abstract

Based on general shell theory and the first order shear deformation theory, an accurate relationship between strains and displacements of a twisted plate is derived by the Green strain tensor. An equation of equilibrium for free vibration is given by the principle of virtual work and the governing equation is solved by using the Rayleigh–Ritz method with sets of orthonormal polynomials in which only the first polynomials are defined according to the geometric boundary conditions of a plate and the others are generated by the Gram–Schmidt process. The numerical verification is carried out by comparing with previous results of cantilever plates. Vibration characteristics of cantilever twisted plates such as frequency parameters and corresponding mode shapes are obtained by the present numerical method, and the effects of the twist angle, the aspect ratio and the thickness ratio on them are studied.

1. Introduction

A plate is one of the most important elements in structural mechanics and has many applications in engineering. Vibration is one of the problems in its dynamics and has attracted researchers' attention. Many studied on linear and non-linear vibration performance of plate [1–5] by the finite element method, the Galerkin method, the Rayleigh–Ritz method, and other methods have been carried out. Most of the previous work on this subject is about vibration characteristics of different plates such as rectangular, circular, elliptical and skew plates with uniform or

*Corresponding author. Tel.: +86-571-883-20-472; fax: +86-571-883-20-130.
E-mail address: kokaka2sakura@hotmail.com (X.X. Hu).

0022-460X/$ - see front matter
doi:10.1016/j.jsv.2003.08.027

non-uniform thickness, and the effects of the boundary conditions and other geometric parameters on their vibration behavior.

Since 1980s the Rayleigh–Ritz method became one of the most popular and powerful approximate approach for analyzing free vibration of plates, but the choice of a set of the admissible functions is considerably important for the accuracy of the Rayleigh–Ritz method. Beam characteristic functions, degenerate beam functions, orthogonal characteristic polynomials or even simple powers of the co-ordinate parameters were often utilized successfully in combination with the Rayleigh–Ritz method for analyzing the vibration of various plates.

In order to seek an exact solution of plates with various boundary conditions, Bhat proposed a method for analyzing rectangular plates using characteristic orthogonal polynomials in the Rayleigh–Ritz method [6]. The Rayleigh–Ritz method with orthogonal polynomials was employed to study the transverse vibration of elliptic and skew plates [7,8], and to study the flexural vibration and buckling of isotropic and orthotropic rectangular plates [9]. It is highlighted that the newly developed *pb*-2 Rayleigh–Ritz method provided the versatile performance in accommodating various boundary conditions [10–12]. More recently, the studies on structural vibration by boundary characteristic orthogonal polynomials using the Rayleigh–Ritz method were reviewed [13].

There were a few studies on the vibration characteristics of twisted plates and influence of geometric parameters on them. The characteristics of twisted cantilever plates such as natural frequencies and mode shapes as well as normalized shear stress distribution were analyzed by using the finite element method and the experimental method called holographic interferometry [14]. To aid in solving the controversy over the widely different results of the free vibration frequencies of cantilever twisted plates obtained by various methods of analysis, the vibration characteristics of the plates were carried out by a joint government/industry/university research group. One of the research papers [15] provided the research results of twisted plates with 20 different geometric configurations which were obtained by the finite element method with plate elements, shell elements and solid elements, and the other methods based on the shell theory and beam theory as well as experimental methods. Based on an accurate relationship of strain–displacement of twisted plates on the thin shell theory, a method was proposed for free vibration analysis of the thin plates by the principle of virtual work in conjunction with the Rayleigh–Ritz method, in which a set of displacement functions was assumed to be general algebraic polynomials satisfying the geometric boundary conditions [16,17]. However, the thin shell theory employed does not ensure the accuracy of the results when the thickness of a plate is not so small as to neglect the influence of transverse shear deformation.

In this paper, the object is to comprehend the free vibration characteristics of twisted plates when the transverse shear deformation and rotary inertia are taken into account. Therefore, an accurate strain–displacement relationship of a twisted plate is derived based on general shell theory and an equation of equilibrium for free vibration is formulated by the principle of virtual work. Applying the Rayleigh–Ritz method with admissible displacement functions which are orthonormal polynomials generated by the Gram–Schmidt process, an eigenfrequency equation of the problem is presented. The vibration frequency parameters and their corresponding mode shapes of cantilever plates are achieved by the present method and the influence of the twist angle, the aspect ratio and the thickness ratio on vibration characteristics is investigated.

2. Mathematical formulation

A configuration of a plate with an uniform rate of twist k around the x-axis is shown in Fig. 1, where the co-ordinates x- and y-axes on the mid-surface of the plate have unit vectors $\mathbf{i}_1$ and $\mathbf{i}_2$, respectively. The unit vector perpendicular to the mid-surface is denoted by $\mathbf{i}_3$ chosen so that $\mathbf{i}_1$, $\mathbf{i}_2$ and $\mathbf{i}_3$ form a right-handed orthogonal co-ordinate system. The z-axis is normal to the mid-surface. The length, the width and the thickness of the plate are represented by a, b and t, respectively. K denotes a twist angle at an end of the plate.

2.1. Strain–displacement relationship

Assuming a local co-ordinates from a point on the mid-surface, $\mathbf{a}_1$ and $\mathbf{a}_2$ are the vectors in their directions and the unit vector $\mathbf{a}_3$ is introduced, which is defined as the following [16]:

$$\mathbf{a}_1 = \mathbf{i}_1 + ky\mathbf{i}_3, \quad \mathbf{a}_2 = \mathbf{i}_2, \quad \mathbf{a}_3 = \frac{\mathbf{a}_1 \times \mathbf{a}_2}{|\mathbf{a}_1 \times \mathbf{a}_2|} = -\frac{ky}{\sqrt{g}}\mathbf{i}_1 + \frac{1}{\sqrt{g}}\mathbf{i}_3, \tag{1}$$

where

$$g = 1 + k^2y^2. \tag{2}$$

The configuration of the twisted plate before and after deformation can be given by the position vectors, respectively,

$$\mathbf{r}^{(0)} = \left(x - \frac{kyz}{\sqrt{g}}\right)\mathbf{i}_1 + y\,\mathbf{i}_2 + \frac{z}{\sqrt{g}}\mathbf{i}_3, \;\; \mathbf{r} = \mathbf{r}^{(0)} + \mathbf{U}, \tag{3}$$

where $\mathbf{U}$ is a displacement vector having components $\mathscr{U}$, $\mathscr{V}$ and $\mathscr{W}$ in $\mathbf{a}_1$, $\mathbf{a}_2$ and $\mathbf{a}_3$, respectively.

According to the Green strain tensor, the suitable strain with respect to (x, y, z) is defined as

$$2f_{ij} = \frac{\partial \mathbf{r}}{\partial \alpha^i} \cdot \frac{\partial \mathbf{r}}{\partial \alpha^j} - \frac{\partial \mathbf{r}^{(0)}}{\partial \alpha^i} \cdot \frac{\partial \mathbf{r}^{(0)}}{\partial \alpha^j} \;(i,\; j = 1,\; 2,\; 3;\; \alpha^1 = x,\; \alpha^2 = y,\; \alpha^3 = z). \tag{4}$$

In order to achieve the engineering strains of the twisted plate, a local rectangular Cartesian co-ordinate system (ξ, η, ζ) with a set of unit vectors $(\mathbf{j}_1, \mathbf{j}_2, \mathbf{j}_3)$ is introduced by

$$\mathbf{j}_1 = \frac{\mathbf{a}_1}{|\mathbf{a}_1|}, \quad \mathbf{j}_2 = \frac{\mathbf{a}_2}{|\mathbf{a}_2|}, \quad \mathbf{j}_3 = \mathbf{a}_3. \tag{5}$$

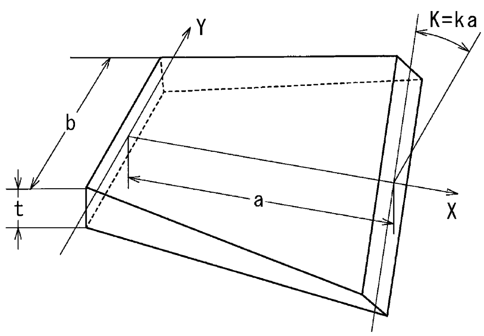

Fig. 1. Geometry and co-ordinates of a twisted plate.

After the transformation, the following strains are obtained:

$$\varepsilon_{\xi\xi} = \frac{1}{F}\left(\sqrt{g}\frac{\partial \mathscr{U}}{\partial x} + zk\frac{\partial \mathscr{U}}{\partial y} + z\frac{k^3 y}{g}\mathscr{U} + \frac{k^2 y}{\sqrt{g}}\mathscr{V} - z\frac{k^2}{g\sqrt{g}}\mathscr{W}\right),$$

$$\varepsilon_{\eta\eta} = \frac{1}{F}\left(-z\frac{k^3 y}{g}\mathscr{U} + z\frac{k}{g}\frac{\partial \mathscr{V}}{\partial x} + \sqrt{g}\frac{\partial \mathscr{V}}{\partial y} - z\frac{k^2}{g\sqrt{g}}\mathscr{W}\right), \quad \varepsilon_{\zeta\zeta} = \frac{\partial \mathscr{W}}{\partial z},$$

$$\gamma_{\xi\eta} = \frac{1}{F}\left(z\frac{k}{\sqrt{g}} + g\frac{\partial \mathscr{U}}{\partial y} + \frac{\partial \mathscr{V}}{\partial x} + z\frac{k}{\sqrt{g}}\frac{\partial \mathscr{V}}{\partial y} + z\frac{k^3 y}{g\sqrt{g}}\mathscr{V} - \frac{2k}{\sqrt{g}}\mathscr{W}\right),$$

$$\gamma_{\xi\zeta} = \frac{1}{F}\left(F\sqrt{g}\frac{\partial \mathscr{U}}{\partial z} + z\frac{k^2}{g}\mathscr{U} + \frac{k}{\sqrt{g}}\mathscr{V} + \frac{\partial \mathscr{W}}{\partial x} + z\frac{k}{\sqrt{g}}\frac{\partial \mathscr{W}}{\partial y}\right),$$

$$\gamma_{\eta\zeta} = \frac{1}{F}\left(k\mathscr{U} + F\frac{\partial \mathscr{V}}{\partial z} + z\frac{k^2}{g\sqrt{g}}\mathscr{V} + z\frac{k}{g}\frac{\partial \mathscr{W}}{\partial x} + \sqrt{g}\frac{\partial \mathscr{W}}{\partial y}\right), \tag{6}$$

where $F = \sqrt{g}(1 - z^2k^2/g^2)$.

To the small displacement theory of a plate, the most natural and simple expression to include the influence of transverse shear deformation is to assume that

$$\mathscr{U} = u + zu_1, \quad \mathscr{V} = v + zv_1, \quad \mathscr{W} = w, \tag{7}$$

where u, v and w denote the linear displacements of a point on the mid-surface, and u_1 and v_1 are angular displacements of the cross-section perpendicular to the mid-surface in the x and y directions, respectively. Applying Eq. (7) and introducing the following non-dimensional indices,

$$U = \frac{u}{a},\ V = \frac{v}{a},\ W = \frac{w}{a},\ U_1 = u_1,\ V_1 = v_1,\ X = \frac{x}{a},\ Y = \frac{y}{b},\ K = ka. \tag{8}$$

Eq. (6) can be rewritten as the matrix form, or

$$\{\varepsilon_{\xi\xi}\ \varepsilon_{\eta\eta}\ \gamma_{\xi\eta}\ \gamma_{\xi\zeta}\ \gamma_{\eta\zeta}\}^{\mathrm{T}} = \frac{1}{F}(\mathscr{L}_1\mathscr{G}^{(1)}\mathscr{R}_1 + \mathscr{L}_2\mathscr{G}^{(2)}\mathscr{R}_2), \tag{9}$$

where the relevant quantities are defined by

$$\mathscr{L}_1 = \begin{bmatrix} 1 & \frac{z}{a} & 0 & 0 & 0 & 0 & 0 & 0 & 0 & 0 \\ 0 & 0 & 1 & \frac{z}{a} & 0 & 0 & 0 & 0 & 0 & 0 \\ 0 & 0 & 0 & 0 & 1 & \frac{z}{a} & 0 & 0 & 0 & 0 \\ 0 & 0 & 0 & 0 & 0 & 0 & 1 & \frac{z}{a} & 0 & 0 \\ 0 & 0 & 0 & 0 & 0 & 0 & 0 & 0 & 1 & \frac{z}{a} \end{bmatrix}, \quad \mathscr{L}_2 = \begin{bmatrix} \frac{z}{a} & \frac{z^2}{a^2} & 0 & 0 & 0 & 0 & 0 & 0 & 0 & 0 \\ 0 & 0 & \frac{z}{a} & \frac{z^2}{a^2} & 0 & 0 & 0 & 0 & 0 & 0 \\ 0 & 0 & 0 & 0 & \frac{z}{a} & \frac{z^2}{a^2} & 0 & 0 & 0 & 0 \\ 0 & 0 & 0 & 0 & 0 & 0 & 1 & \frac{z}{a} & 0 & 0 \\ 0 & 0 & 0 & 0 & 0 & 0 & 0 & 0 & 1 & \frac{z}{a} \end{bmatrix},$$

$$\mathscr{R}_1^{\mathrm{T}} = \left\{ \frac{\partial U}{\partial X} \quad \frac{\partial U}{\partial Y} \quad U \quad \frac{\partial V}{\partial X} \quad \frac{\partial V}{\partial Y} \quad V \quad \frac{\partial W}{\partial X} \quad \frac{\partial W}{\partial Y} \quad W \right\},$$

$$\mathscr{R}_2^{\mathrm{T}} = \left\{ \frac{\partial U_1}{\partial X} \quad \frac{\partial U_1}{\partial Y} \quad U_1 \quad \frac{\partial V_1}{\partial X} \quad \frac{\partial V_1}{\partial Y} \quad V_1 \right\}, \tag{10}$$

and the matrices $\mathscr{G}^{(1)}$ and $\mathscr{G}^{(2)}$ are given in Appendix A.

The constitutive relationship between strains and stresses for the homogeneous plates can be written as

$$\sigma = \begin{Bmatrix} \sigma_{\xi\xi} \\ \sigma_{\eta\eta} \\ \tau_{\xi\eta} \\ \tau_{\xi\zeta} \\ \tau_{\eta\zeta} \end{Bmatrix} = \begin{bmatrix} \frac{E}{1-v^2} & \frac{vE}{1-v^2} & 0 & 0 & 0 \\ \frac{vE}{1-v^2} & \frac{E}{1-v^2} & 0 & 0 & 0 \\ 0 & 0 & G & 0 & 0 \\ 0 & 0 & 0 & \beta G & 0 \\ 0 & 0 & 0 & 0 & \beta G \end{bmatrix} \begin{Bmatrix} \varepsilon_{\xi\xi} \\ \varepsilon_{\eta\eta} \\ \gamma_{\xi\eta} \\ \gamma_{\xi\zeta} \\ \gamma_{\eta\zeta} \end{Bmatrix} = \mathscr{D}\varepsilon, \tag{11}$$

where E, v and G are Young's modulus, the Poisson ratio and shear modulus, respectively, and β is a shear correction factor.

2.2. Governing equation of vibration

The equation of equilibrium for free vibration is shown as the following by the principle of virtual work,

$$\delta\Pi = \int\int\int_{vol} \varepsilon^{\mathrm{T}} \delta\sigma \, \mathrm{d}V_{ol} - \int\int\int_{vol} \rho\omega^2 \mathbf{U}\delta\mathbf{U} \, \mathrm{d}V_{ol}, \tag{12}$$

where ω denotes an angular frequency of vibration and ρ is a density of a material.

Substituting the related quantities into Eq. (12), multiplying a^2/D and integrating with respect to z yields

$$\begin{aligned} \delta\Pi = & \int\int_A \{\mathscr{R}_1^{\mathrm{T}} \;\; \mathscr{R}_2^{\mathrm{T}}\} \begin{bmatrix} \{\mathscr{G}^{(1)}\}^{\mathrm{T}} \mathscr{D}^{(1)} \mathscr{G}^{(1)} & \{\mathscr{G}^{(1)}\}^{\mathrm{T}} \mathscr{D}^{(2)} \mathscr{G}^{(2)} \\ \{\mathscr{G}^{(2)}\}^{\mathrm{T}} \{\mathscr{D}^{(2)}\}^{\mathrm{T}} \mathscr{G}^{(1)} & \{\mathscr{G}^{(2)}\}^{\mathrm{T}} \mathscr{D}^{(3)} \mathscr{G}^{(2)} \end{bmatrix} \begin{Bmatrix} \delta\mathscr{R}_1^{\mathrm{T}} \\ \delta\mathscr{R}_2^{\mathrm{T}} \end{Bmatrix} \mathrm{d}X \, \mathrm{d}Y \\ & - \lambda^2 \int\int_A \{U \;\; V \;\; W \;\; U_1 \;\; V_1\} \mathscr{B} \{\delta U \;\; \delta V \;\; \delta W \;\; \delta U_1 \;\; \delta V_1\}^{\mathrm{T}} \, \mathrm{d}X \, \mathrm{d}Y, \end{aligned} \tag{13}$$

in which the matrices $\mathscr{D}^{(1)}$, $\mathscr{D}^{(2)}$, $\mathscr{D}^{(3)}$ and $\mathscr{B}$ are defined by

$$\mathscr{D}^{(1)} = \int_{-t/2}^{t/2} \frac{1}{F} \frac{a^2}{D} \mathscr{L}_1^{\mathrm{T}} \mathscr{D} \mathscr{L}_1 \, \mathrm{d}z, \quad \mathscr{D}^{(2)} = \int_{-t/2}^{t/2} \frac{1}{F} \frac{a^2}{D} \mathscr{L}_2^{\mathrm{T}} \mathscr{D} \mathscr{L}_1 \, \mathrm{d}z, \quad \mathscr{D}^{(3)} = \int_{-t/2}^{t/2} \frac{1}{F} \frac{a^2}{D} \mathscr{L}_2^{\mathrm{T}} \mathscr{D} \mathscr{L}_2 \, \mathrm{d}z,$$

$$\mathscr{B} = diag\{B_{11} \;\; B_{22} \;\; \cdots \;\; B_{55}\} = diag\left\{ g\sqrt{g} \quad \sqrt{g} \quad \sqrt{g} \quad \frac{g\sqrt{g}t^2}{12a^2} \quad \frac{\sqrt{g}t^2}{12a^2} \right\}, \tag{14}$$

and λ is a frequency parameter given as

$$\lambda^2 = \frac{\rho\omega^2 t a^4}{D}, \quad D = \frac{Et^3}{12(1-\nu^2)}. \tag{15}$$

Considering a set of characteristic orthonormal polynomials in the Rayleigh–Ritz method, the three linear displacement functions U, V and W, and the two angular displacement functions U_1 and V_1 are defined as follows:

$$U = \sum_{i=1}^{N_U} \sum_{j=1}^{M_U} a_{ij}^U \, \Phi_i^U(X) \, \Psi_j^U(Y), \quad V = \sum_{k=1}^{N_V} \sum_{l=1}^{M_V} a_{kl}^V \, \Phi_k^V(X) \, \Psi_l^V(Y),$$

$$W = \sum_{m=1}^{N_W} \sum_{n=1}^{M_W} a_{mn}^W \, \Phi_m^W(X) \, \Psi_n^W(Y),$$

$$U_1 = \sum_{p=1}^{N_{U_1}} \sum_{q=1}^{M_{U_1}} a_{pq}^{U_1} \Phi_p^{U_1}(X) \Psi_q^{U_1}(Y), \quad V_1 = \sum_{r=1}^{N_{V_1}} \sum_{s=1}^{M_{V_1}} a_{rs}^{V_1} \Phi_r^{V_1}(X) \Psi_s^{V_1}(Y), \tag{16}$$

where $a_{PQ}^S (S = U, V, W, U_1, V_1; \; P, Q = 1, 2, 3, \ldots)$ are unknown coefficients, and $\Phi_P^S(X)$ and $\Psi_Q^S(Y)$ are polynomials generated by the Gram–Schmidt process. For example, the first polynomial $\Phi_1(X)$ is given so that it satisfies a geometric boundary conditions of the plate, and a set of orthogonal polynomials within $[X_1, \; X_2]$ can be obtained by the following recursive algorithm,

$$\Phi_2(X) = (X - B_2)\Phi_1(X), \quad \Phi_P(X) = (X - B_P)\Phi_{P-1}(X) - C_P \Phi_{P-2}(X) \quad (P = 3, 4, 5, \ldots),$$

$$B_P = \int_{X_1}^{X_2} \Gamma_X \Phi_{P-1}^2(X) X \, \mathrm{d}X \bigg/ \int_{X_1}^{X_2} \Gamma_X \Phi_{P-1}^2(X) \, \mathrm{d}X,$$

$$C_P = \int_{X_1}^{X_2} \Gamma_X \Phi_{P-1}(X) \Phi_{P-2}(X) X \, \mathrm{d}X \bigg/ \int_{X_1}^{X_2} \Gamma_X \Phi_{P-2}^2(X) \, \mathrm{d}X, \tag{17}$$

where Γ_X is a weighting function and the polynomial $\Phi_P(X)$ satisfies the orthogonal condition

$$\int_{X_1}^{X_2} \Gamma_X \Phi_P(X) \Phi_Q(X) \, \mathrm{d}X = \begin{cases} 0 & \text{if } P \neq Q, \\ \delta_{PQ} & \text{if } P = Q. \end{cases} \tag{18}$$

If the unit weighting function Γ_X is used and the coefficients of the orthogonal polynomials are re-defined by

$$\int_{X_1}^{X_2} \Phi_P^2(X) \, \mathrm{d}X = 1, \tag{19}$$

then a set of orthonormal polynomials $\Phi_P(X)$ $(P = 1, \; 2, \; 3, \ldots)$ is achieved.

Substituting Eq. (16) into Eq. (13) and considering the following requirement due to the independent orthonormal polynomials:

$$\frac{\partial}{\partial a_{PQ}^S} \delta \Pi = 0 \; (S = U, V, W, U_1, V_1; P, Q = 1, 2, 3, \ldots), \tag{20}$$

a set of simultaneous linear algebraic equations for free vibration of the twisted plate is obtained as follows:

$$\left\{\begin{bmatrix}\mathbf{K}^{(11)} & \mathbf{K}^{(12)} & \cdots & \mathbf{K}^{(15)}\\ & \mathbf{K}^{(22)} & \cdots & \mathbf{K}^{(25)}\\ & & \ddots & \vdots\\ Sym & & & \mathbf{K}^{(55)}\end{bmatrix} - \lambda^2\begin{bmatrix}\mathbf{M}^{(11)} & & & \mathbf{0}\\ & \mathbf{M}^{(22)} & & \\ & & \ddots & \\ \mathbf{0} & & & \mathbf{M}^{(55)}\end{bmatrix}\right\}\begin{Bmatrix}\mathbf{a}^U\\ \mathbf{a}^V\\ \mathbf{a}^W\\ \mathbf{a}^{U_1}\\ \mathbf{a}^{V_1}\end{Bmatrix} = \{\mathbf{0}\}, \quad (21)$$

where the elements in the sub-stiffness matrices $\mathbf{K}^{(ij)}$ and the sub-mass matrices $\mathbf{M}^{(ii)}$ are

$$K_{pq}^{(ij)} = \int\int_A \left\{ \frac{\partial \Phi_m^i(X)}{\partial X}\Psi_n^i(Y) \quad \Phi_m^i(X)\frac{\partial \Psi_n^i(Y)}{\partial Y} \quad \Phi_m^i(X)\Psi_n^i(Y)\right\}\mathscr{Q}^{(ij)}$$
$$\cdot\left\{ \frac{\partial \Phi_r^j(X)}{\partial X}\Psi_s^j(Y) \quad \Phi_r^j(X)\frac{\partial \Psi_s^j(Y)}{\partial Y} \quad \Phi_r^j(X)\Psi_s^j(Y)\right\}^{\mathrm{T}} \mathrm{d}X\,\mathrm{d}Y,$$
$$M_{pq}^{(ii)} = \int\int_A B_{ii}\Phi_m^i(X)\Psi_n^i(Y)\Phi_r^i(X)\Psi_s^i(Y)\,\mathrm{d}X\,\mathrm{d}Y,$$
$$(i,j = 1,2,\ldots,5; \quad p,q = 1,2,3,\ldots; \quad m,n,r,s = 1,2,3,\ldots). \quad (22)$$

The superscripts i and j denote the different displacement functions, or their values from 1 to 5 are corresponding to U, V, W, U_1 and V_1, respectively, and

$$\begin{bmatrix}\mathscr{Q}^{(11)} & \mathscr{Q}^{(12)} & \cdots & \mathscr{Q}^{(15)}\\ & \mathscr{Q}^{(22)} & \cdots & \mathscr{Q}^{(25)}\\ & & \ddots & \vdots\\ Sym & & & \mathscr{Q}^{(55)}\end{bmatrix} = \begin{bmatrix}\{\mathscr{G}^{(1)}\}^{\mathrm{T}}\mathscr{D}^{(1)}\mathscr{G}^{(1)} & \{\mathscr{G}^{(1)}\}^{\mathrm{T}}\mathscr{D}^{(2)}\mathscr{G}^{(2)}\\ \{\mathscr{G}^{(2)}\}^{\mathrm{T}}\{\mathscr{D}^{(2)}\}^{\mathrm{T}}\mathscr{G}^{(1)} & \{\mathscr{G}^{(2)}\}^{\mathrm{T}}\mathscr{D}^{(3)}\mathscr{G}^{(2)}\end{bmatrix}. \quad (23)$$

For the non-trivial solutions of Eq. (21), a governing equation can be obtained, namely:

$$|\mathbf{K} - \lambda^2\mathbf{M}| = \mathbf{0}, \quad (24)$$

and the eigenvalues and eigenvectors can be solved from the equation easily.

3. Convergence and comparison

Cantilever twisted plates, which have a fixed edge and three free others, are considered as an example of numerical analysis in this paper, and the unit weighting functions Γ_X and Γ_Y are used, that is to say that the first polynomials with respect to X and Y for the five displacement functions can be defined by

$$\Phi_1^U(X) = \Phi_1^V(X) = \Phi_1^W(X) = \Phi_1^{U_1}(X) = \Phi_1^{V_1}(X) = \sqrt{3}X \quad (X\in[0,\ 1]),$$
$$\Psi_1^U(Y) = \Psi_1^V(Y) = \Psi_1^W(Y) = \Psi_1^{U_1}(Y) = \Psi_1^{V_1}(Y) = 1 \quad (Y\in[-1/2,\ 1/2]). \quad (25)$$

The free vibration of twisted plates is represented by a governing equation (24) where the Rayleigh–Ritz method with orthonormal polynomials and the Gauss–Legendre numerical integration are utilized. The number of terms of orthonormal polynomials in each of the admissible displacement functions and the number of integration points affect not only the accuracy of results but also the efficiency of calculation. The convergence and the accuracy are improved with more terms of orthonormal polynomials and more points of Gauss–Legendre integration, but too many calculations might cause numerical errors. From experience it was known that a 12-point Gauss–Legendre numerical integration would yield better results. In the following, the effect of the number of terms in the displacement functions on frequency parameters is investigated and then the proper numbers are determined. Poisson's ratio ν is assumed to be 0.3 and the shear correction factor β is $\pi^2/12$.

3.1. Convergence study on frequency parameters

There are five displacement functions, each of which is constructed by two independent sets of orthonormal polynomials with respect to X and Y, respectively. For any displacement function, there are no restrictions on the choice of terms in the two sets of orthonormal polynomials $\{\Phi(X)\}$ and $\{\Psi(X)\}$. There are no coupling terms among the five displacement functions too. From Eq. (16), it is known that Eq. (21) is a set of $N_U \times M_U + N_V \times M_V + N_W \times M_W + N_{U_1} \times M_{U_1} + N_{V_1} \times M_{V_1}$ simultaneous linear algebraic equations. For the convenience, the following relationships are defined

$$N_U = M_U - 1 = N_V = M_V - 1 = N_W = M_W - 1 = N_1,$$
$$N_{U_1} = M_{U_1} - 1 = N_{V_1} = M_{V_1} - 1 = N_2. \quad (26)$$

Table 1
Convergence study on $\lambda(\omega a^2\sqrt{\rho t/D})$ for plates with $a/b = 1.0$ and $t/b = 0.01$

K	N_1, N_2 Terms		7,9 56/90	7,11 56/132	9,7 90/56	11,7 132/56	8,8 72/72	9,9 90/90	10,10 110/110	11,11 132/132
30°	λ_i	1	3.4142	3.4140	3.4140	3.4138	3.4133	3.4130	3.4126	3.4126
		2	19.159	19.158	19.157	19.156	19.155	19.154	19.152	19.151
		3	49.420	49.416	49.389	49.387	49.389	49.378	49.376	49.372
		4	50.160	50.155	50.074	50.072	50.075	50.069	50.063	50.062
		5	57.915	57.912	57.786	57.784	57.782	57.765	57.758	57.757
		6	75.967	75.949	75.873	75.872	75.859	75.820	75.813	75.803
		7	94.305	94.293	94.238	94.234	94.238	94.193	94.187	94.176
		8	106.13	106.08	105.75	105.75	105.70	105.65	105.60	105.60
		9	111.22	111.19	111.12	111.11	111.08	110.96	110.95	110.93
		10	120.60	120.47	114.55	114.55	114.82	114.47	114.29	114.28
60°	λ_i	1	3.2462	3.2460	3.2458	3.2457	3.2450	3.2446	3.2443	3.2442
		2	14.631	14.630	14.629	14.629	14.627	14.626	14.624	14.624
		3	49.018	49.015	48.715	48.714	48.712	48.697	48.691	48.691
		4	66.135	66.126	65.967	65.963	65.961	65.877	65.869	65.862
		5	74.004	73.984	73.374	73.367	73.513	73.265	73.253	73.248
		6	106.54	106.44	101.22	101.22	102.15	101.14	100.99	100.98
		7	108.60	108.57	108.25	108.25	108.23	107.96	107.90	107.88
		8	140.21	140.17	139.63	139.62	139.59	138.99	138.90	138.85
		9	145.21	145.14	144.60	144.59	144.60	144.30	144.01	143.97
		10	152.46	152.32	147.73	147.71	148.81	146.70	146.56	146.50

Cantilever plates with two twist angles $K = 30^\circ$ and 60°, an aspect ratio $a/b = 1.0$ and a thickness ratio $t/b = 0.01$ are selected and the numerical results are shown in Table 1 by using the present method for several combinations of the number of terms (N_1, N_2). It is observed that the frequency parameters of the plate with small twist angle converge better than those with large twist angle, and the lower frequency parameters converge faster than the higher ones. As the (N_1, N_2) is taken to be $(9, 9)$, $(10, 10)$ and $(11, 11)$, the maximum deviation in the higher frequency parameters is less than 0.3%. Considering the efficiency of calculation $(9, 9)$ is utilized in the following analyses.

3.2. Comparison with previous methods

Firstly, the plates with CFFF boundary condition on the Mindlin plate theory [12] is considered which have aspect ratios $a/b = 0.4$, 1.0 and 1.5, and thickness ratios $t/b = 0.001$, 0.050 and 0.100. The first eight frequency parameters $\lambda = (\omega b^2/\pi^2)\sqrt{\rho t/D}$ obtained by the two methods

Table 2
Comparison of $\lambda(\omega b^2/\pi^2\sqrt{\rho t/D})$ for plates with $K = 0^\circ$ [5]

a/b	t/b	Method	No. of vibration mode							
			1	2	3	4	5	6	7	8
0.4	0.001	Liew	2.215	3.019	5.108	8.741	13.628	14.593	14.925	18.192
		Present	2.2150	3.0197	5.1101	8.7424	13.635	14.613	14.928	18.201
	0.050	Liew	2.182	2.914	4.839	8.191	12.517	13.443	13.557	16.224
		Present	2.1824	2.9147	4.8459	8.1978	12.526	13.464	13.561	16.240
	0.100	Liew	2.099	2.727	4.387	7.253	10.399	11.130	11.424	13.148
		Present	2.0995	2.7271	4.3882	7.2537	10.400	11.132	11.432	13.152
1.0	0.001	Liew	0.352	0.862	2.157	2.756	3.136	5.490	6.206	6.499
		Present	0.3515	0.8621	2.1566	2.7558	3.1371	5.4911	6.2072	6.4990
	0.050	Liew	0.350	0.844	2.121	2.698	3.039	5.246	5.989	6.270
		Present	0.3504	0.8449	2.1220	2.7008	3.0428	5.2571	5.9907	6.2739
	0.100	Liew	0.348	0.816	2.034	2.582	2.860	4.811	5.477	5.772
		Present	0.3476	0.8165	2.0346	2.5828	2.8602	4.8130	5.4775	5.7724
1.5	0.001	Liew	0.155	0.525	0.967	1.771	2.411	2.775	3.612	3.842
		Present	0.1553	0.5250	0.9668	1.7715	2.4110	2.7752	3.6132	3.8424
	0.050	Liew	0.155	0.515	0.959	1.730	2.374	2.728	3.506	3.718
		Present	0.1552	0.5158	0.9594	1.7332	2.3754	2.7291	3.5122	3.7260
	0.100	Liew	0.154	0.501	0.940	1.662	2.292	2.612	3.298	3.494
		Present	0.1545	0.5015	0.9404	1.6626	2.2920	2.6127	3.3002	3.4961

Table 3
Comparison of $\lambda(\omega a^2\sqrt{\rho t/D})$ for thin plates with $a/b = 1.0$ [17]

t/b	K	Method	No. of vibration mode									
			1	2	3	4	5	6	7	8	9	10
0.01	0°	Tsuiji	3.4717	8.5089	21.290	27.199	30.964	54.197	61.263	64.143	70.985	92.933
		Present	3.4708	8.4976	21.273	27.173	30.911	54.077	61.169	64.039	70.830	92.668
	30°	Tsuiji	3.4139	19.168	49.410	50.100	57.850	75.905	94.272	105.81	111.15	114.78
		Present	3.4130	19.154	49.379	50.068	57.766	75.820	94.194	105.65	110.96	114.47
	60°	Tsuiji	3.2454	14.637	48.767	65.926	73.319	101.40	108.09	139.17	144.55	146.94
		Present	3.2446	14.626	48.697	65.877	73.265	101.14	107.96	138.99	144.30	146.70
0.05	0°	Tsuiji	3.4722	8.5100	21.292	27.200	30.968	43.519	54.201	61.284	64.159	71.014
		Present	3.4587	8.3388	20.943	26.655	30.031	43.512	51.885	59.126	61.921	67.905
	30°	Tsuiji	3.4045	14.440	18.749	27.213	34.871	46.426	56.321	60.802	63.935	70.763
		Present	3.3915	14.329	18.464	26.735	34.085	46.007	54.282	59.110	61.807	67.945
	60°	Tsuiji	3.2302	14.279	21.832	28.056	41.036	45.746	55.604	63.320	67.481	69.415
		Present	3.2182	14.069	21.723	27.676	40.383	44.638	54.381	61.452	66.325	67.198

are shown in Table 2. Regardless of the aspect ratio and the thickness ratio of the plates, the present first eight λ are in very close agreement with those given by the reference, which demonstrates the accuracy of the present method and the suitability of the terms (N_1, N_2) utilized in the present method although the un-twisted plates are analyzed. It should be noted that only the transverse vibration of plate was studied in the reference and both the transverse and the in-plane vibration of twisted plates are included in this paper. Therefore, the frequency parameters in the table are a part of the results which correspond to the transverse vibration by the present method.

Secondly, the cantilever twisted thin plates with three twist angles $K = 0°, 30°$ and $60°$, two thickness ratios $t/b = 0.05$ and 0.01, and an aspect ratio $a/b = 1.0$ [17] are considered. The method in the reference is based on the classical thin shell theory. The numerical results are given in Table 3. It is observed that the present results are smaller than those in the reference for the plates with different combinations of K and t/b, because the stiffness of plates decreases when transverse shear deformation is included. The first 10 frequency parameters obtained by the two different methods show good agreement in the case of $t/b = 0.01$ with a maximum difference less than 0.3%. Deviations appear in the case of $t/b = 0.05$ but the maximum one is less than 5%, which is brought by transverse shear deformation and rotary inertia due to an increase in thickness. It is verified that the method on the thin shell theory [17] is adequate to the thin twisted plates and has a good accuracy. A recommendation that the influence of the transverse shear deformation may not be neglected when a thickness ratio t/b of a cantilever twisted plate is greater than 0.05 should be considered.

4. Numerical analysis of vibration characteristics

The vibration of various cantilever plates with different twist angles, aspect ratios and thickness ratios is studied in this section. The frequency parameters and the mode shapes of vibration are presented so as to reveal the vibration characteristics and the influence of the parameters. For the given aspect ratios $a/b = 0.5,\ 1.0$ and 2.0, and the combinations of the twist angle K and the thickness ratio t/b, the vibration frequency parameters and some of their mode shapes of plates are obtained by the present numerical analysis.

In Table 4, all the frequency parameters show a downward trend as the thickness ratio t/b increases, and the variations of the frequency parameters for higher modes are much greater than those of the lower ones for the plates with a given twist angle, which becomes large as K increases. It is observed that the first λ shows monotonic decrease with the twist angle K increasing for all cases of t/b. However, there are no simple variations found for the other frequency parameters. The first ten mode shapes of vibration corresponding to nine cases of the plates given by Table 4 are plotted in Fig. 2 (the heavier lines are the nodal lines whose displacement W is zero) where the changes in the mode shapes with the parameters K and t/b are shown. The first vibration modes of all the plates are the first bending mode. The phenomenon implies that an increase in the twist

Table 4
Frequency parameters $\lambda(\omega a^2\sqrt{\rho t/D})$ of plates with $a/b = 0.5$

		No. of vibration mode									
K	t/b	1	2	3	4	5	6	7	8	9	10
0°	0.0125	3.4905	5.3344	10.144	18.992	21.757	24.539	31.204	33.892	42.690	52.628
	0.025	3.4833	5.2955	10.046	18.770	21.511	24.189	30.616	33.386	41.676	51.578
	0.05	3.4579	5.1924	9.7579	18.090	20.623	23.052	27.030	28.851	31.729	38.710
	0.10	3.3688	4.9146	8.9953	13.515	16.256	17.965	19.924	24.441	25.121	27.398
15°	0.0125	3.4171	14.117	17.662	20.711	23.172	31.466	34.766	38.766	48.351	53.913
	0.025	3.4093	8.8916	12.383	19.776	20.356	25.314	31.263	34.150	42.654	51.598
	0.05	3.3843	6.2629	10.253	18.140	19.153	22.741	27.177	29.400	31.635	38.508
	0.10	3.2979	5.1148	8.9949	12.968	16.090	17.983	19.424	24.155	24.572	27.143
30°	0.0125	3.2134	17.981	20.215	25.043	28.489	41.343	44.204	48.484	52.679	56.821
	0.025	3.2058	12.591	16.023	17.642	21.295	28.489	32.351	36.012	44.934	49.220
	0.05	3.1828	7.9446	11.212	16.343	18.044	22.130	26.199	30.747	31.660	38.001
	0.10	3.1039	5.4957	8.9304	11.742	15.556	17.589	18.221	23.094	23.521	26.479
45°	0.0125	2.9329	14.935	22.643	27.366	30.975	44.117	48.786	52.185	55.068	55.232
	0.025	2.9252	14.073	14.589	18.032	21.646	32.056	33.012	37.540	42.844	44.735
	0.05	2.9040	8.8873	11.827	13.578	17.215	21.955	24.548	30.599	32.461	37.061
	0.10	2.8344	5.7448	8.6431	10.425	14.468	16.482	17.043	21.117	22.698	25.579
60°	0.0125	2.6312	12.166	22.694	27.166	31.181	37.746	49.825	49.885	56.533	58.903
	0.025	2.6234	11.870	14.189	18.333	20.989	32.055	34.347	36.486	38.790	39.222
	0.05	2.6038	9.0693	10.866	12.212	15.766	22.176	22.739	30.062	31.075	33.452
	0.10	2.5428	5.7728	7.9511	9.3864	12.899	15.067	16.227	19.113	21.597	24.316

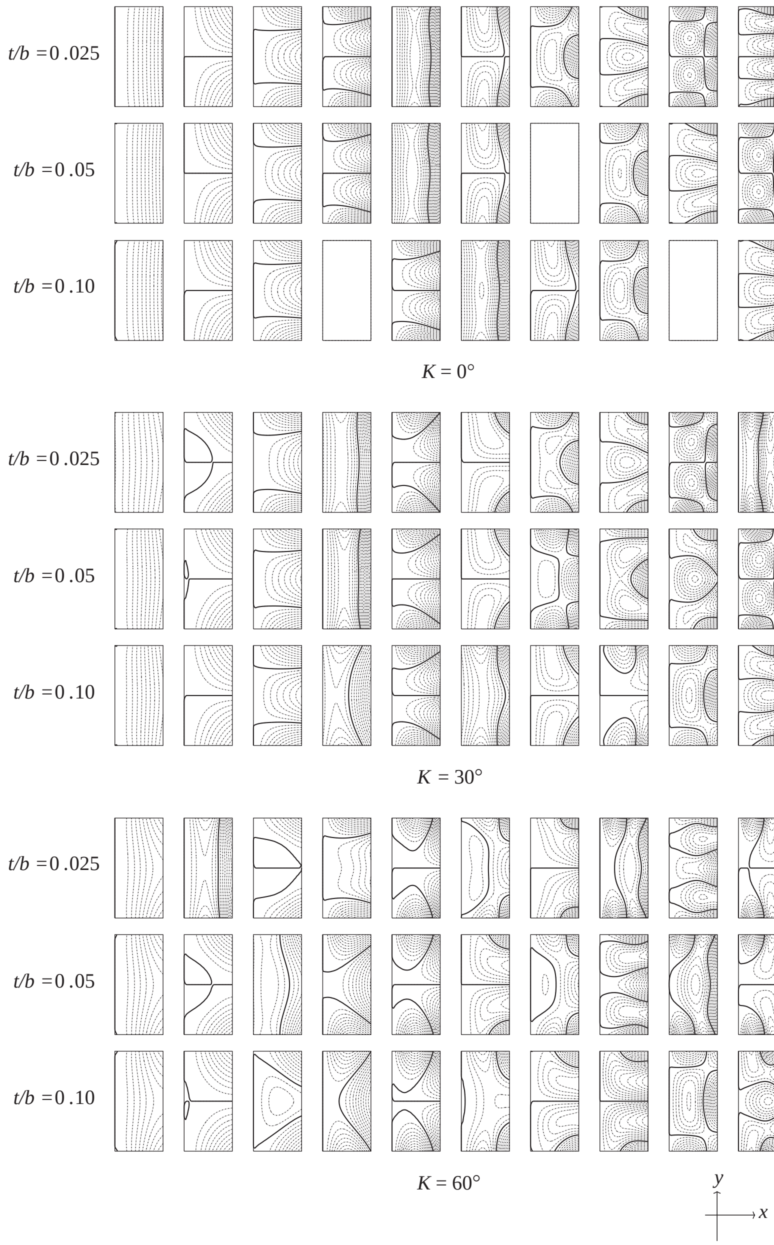

Fig. 2. Vibration mode shapes of plates ($a/b = 0.5$).

angle leads to a reduction in the bending stiffness. It is apparent that the change in mode shapes for the un-twisted plates is different from that for the twisted plates as the thickness ratio varies. In the case of $K = 0^\circ$, there are no in-plane vibration modes in the first ten ones for the thin plate ($t/b = 0.025$) and the different modes appear in order. As the thickness increases, in-plane modes appear which insert into the original sequence of mode shapes of the thin plate. The greater the

Table 5
Frequency parameters $\lambda(\omega a^2\sqrt{\rho t/D})$ of plates with $a/b = 1.0$

K	t/b	No. of vibration mode									
		1	2	3	4	5	6	7	8	9	10
0°	0.0125	3.4704	8.4917	21.264	27.158	30.882	54.010	61.115	63.981	70.745	92.518
	0.025	3.4675	8.4511	21.194	27.043	30.675	53.506	60.692	63.522	70.099	87.024
	0.05	3.4587	8.3388	20.943	26.655	30.031	43.512	51.885	59.126	61.921	67.905
	0.10	3.4305	8.0585	20.081	21.756	25.491	28.229	47.503	52.202	54.060	56.971
15°	0.0125	3.4568	20.855	25.408	32.542	47.385	59.891	67.893	68.103	80.496	102.94
	0.025	3.4512	14.898	20.652	28.195	35.754	56.872	59.465	64.327	72.157	89.870
	0.05	3.4414	10.313	20.267	26.578	31.199	44.412	52.775	58.811	61.891	67.934
	0.10	3.4130	8.5465	18.545	22.720	26.013	28.343	47.516	51.974	52.704	56.713
30°	0.0125	3.4109	19.127	42.477	43.466	57.368	67.128	82.375	92.294	99.260	113.59
	0.025	3.4032	18.960	24.546	31.283	45.737	56.414	64.935	66.680	77.276	96.020
	0.05	3.3915	14.329	18.464	26.735	34.085	46.007	54.282	59.110	61.807	67.945
	0.10	3.3625	9.7555	16.389	23.227	27.435	28.635	47.527	50.135	51.297	55.941
45°	0.0125	3.3364	16.850	51.200	52.430	56.471	81.226	102.17	106.00	114.28	116.38
	0.025	3.3279	16.710	32.426	34.967	52.750	54.547	70.659	73.421	82.901	99.856
	0.05	3.3145	16.223	18.381	27.201	37.464	46.412	54.253	61.670	62.298	67.754
	0.10	3.2845	11.217	14.361	23.173	28.927	28.980	46.864	47.925	50.189	54.661
60°	0.0125	3.2446	14.626	48.697	65.877	73.265	101.14	107.96	138.99	144.30	146.70
	0.025	3.2332	14.488	37.702	38.033	48.910	60.622	75.718	79.619	87.274	97.788
	0.05	3.2182	14.069	21.723	27.676	40.383	44.638	54.381	61.452	66.325	67.198
	0.10	3.1870	12.563	12.591	22.860	29.249	29.879	44.115	47.710	48.687	52.885

thickness is, the easier the in-plane modes occur. For example, the seventh mode ($\lambda = 27.030$) is an in-plane one in the case of $t/b = 0.05$, and the fourth ($\lambda = 13.515$) and ninth ($\lambda = 25.121$) modes are in-plane ones in the case of $t/b = 0.10$. Incorporating Table 4, it is found that the appearance of in-plane modes makes its frequency parameters change greatly. For instance, the variations of the eighth, ninth and tenth frequency parameters are greater than those of the others in the case of $t/b = 0.05$; the same can be seen in the case of $t/b = 0.10$. From the investigation of the un-twisted plates with $a/b = 0.5$, it is known that an increase in transverse shear deformation has little influence on mode shapes. For the plates with $K = 30°$ and $60°$, although in-plane modes are not found, the changes in mode shapes can be observed as the thickness ratio varies in Fig. 2 where the mode shapes change and switch with each other as well as new modes appear. In other words, the effects of the transverse shear deformation on mode shapes show differences for different modes and different twist angles of cantilever plates. For example, there are no changes in the first, third and fifth mode shapes, the second mode becomes the first torsional one, some switch with each other, and the others show the complicated changes in the case of $K = 30°$ as the thickness ratio increases. In the case of $K = 60°$, except for small changes in the first and fifth modes, large changes occur in the others. It is known that the effect of the transverse shear

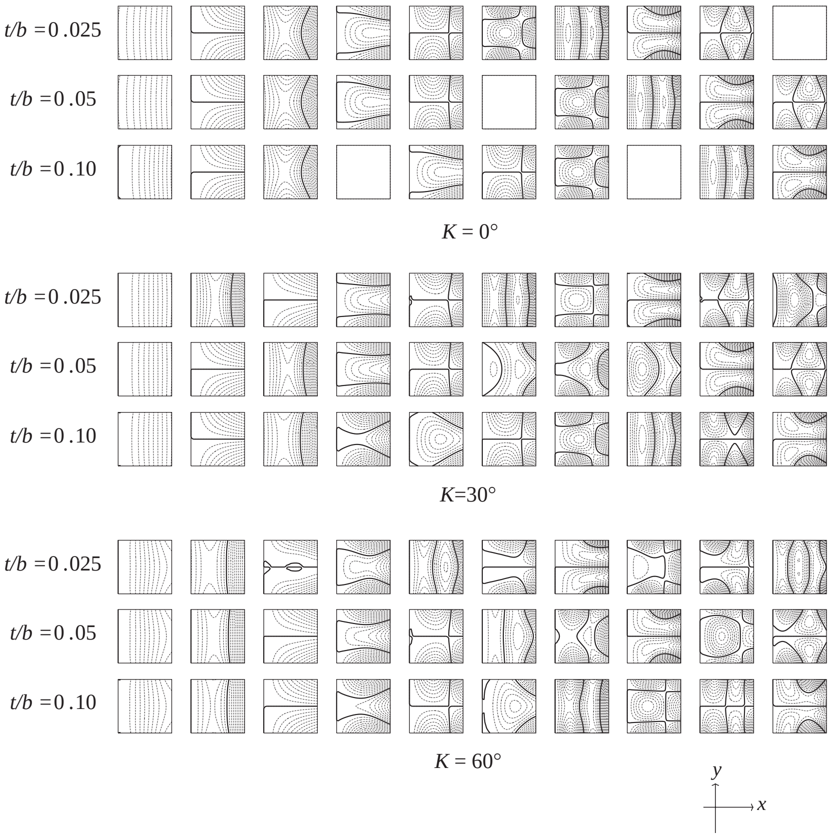

Fig. 3. Vibration mode shapes of plates ($a/b = 1.0$).

deformation on mode shapes is influenced by the twist angle. Also, it can be observed in Fig. 2 that the mode shapes vary with the twist angle.

The cantilever square plates are investigated, and the frequency parameters and some mode shapes of vibration are given in Table 5 and Fig. 3, respectively. Comparing with the results in Table 4, it is found that most of the frequency parameters are greater, especially for the higher frequency parameters of highly twisted thin plates, which means that the global stiffness of the plate ($a/b = 1.0$) is greater than that of the plate ($a/b = 0.5$). For an example of the tenth frequency parameters of the plates, the differences are 75.80% and 149.05% in the cases of $K = 0°$ and 60°. From the mode shapes of the un-twisted plates in Fig. 3, there are no changes in mode shapes except that the in-plane modes appear with the thickness ratio. In the case of $K = 30°$, it is obvious that mode shapes switch with each other such as the second bending and first torsional modes while t/b varies from 0.025 to 0.05, the eighth mode becomes ninth one and then tenth one with t/b from 0.025 to 0.05 then to 0.10, although this is accompanied by a little distortion. In the case of $K = 60°$, there are complex changes in mode shapes with t/b. As to the influence of the twist angle on mode shapes, it is observed that the main representation is an exchange of mode shapes as K is small, and an exchange accompanying with distortion as K is

Table 6
Frequency parameters $\lambda(\omega a^2\sqrt{\rho t/D})$ of plates with $a/b = 2.0$

K	t/b	No. of vibration mode									
		1	2	3	4	5	6	7	8	9	10
0°	0.0125	3.4396	14.779	21.430	48.103	60.117	92.369	93.025	118.48	126.76	152.69
	0.025	3.4378	14.717	21.409	47.896	59.995	91.933	92.793	114.93	118.03	126.14
	0.05	3.4335	14.555	21.337	47.300	57.462	59.557	90.545	91.953	116.40	124.07
	0.10	3.4224	14.185	21.088	28.731	45.751	58.008	86.505	89.106	104.27	109.59
15°	0.0125	3.4402	20.825	31.526	59.406	83.293	94.573	118.00	124.86	136.70	176.48
	0.025	3.4361	20.323	20.776	58.917	59.133	92.558	101.12	112.26	123.72	130.07
	0.05	3.4312	16.131	20.644	50.218	56.197	61.917	92.048	92.764	116.18	124.46
	0.10	3.4198	14.571	20.010	30.099	46.420	57.513	86.906	88.989	104.15	107.97
30°	0.0125	3.4389	19.258	56.270	57.429	98.911	115.54	136.61	162.32	182.31	195.17
	0.025	3.4310	19.170	31.196	56.949	82.390	92.477	110.55	123.35	129.97	143.71
	0.05	3.4243	18.944	20.002	54.317	57.863	66.460	92.342	98.917	115.45	125.78
	0.10	3.4123	15.642	17.951	32.938	48.322	56.193	88.066	88.638	103.81	106.01
45°	0.0125	3.4335	17.267	54.675	80.257	105.45	111.98	182.31	191.66	195.44	231.86
	0.025	3.4226	17.163	42.917	54.102	93.103	108.05	108.37	138.67	150.04	161.20
	0.05	3.4137	16.902	24.878	52.018	68.095	71.673	92.828	107.79	114.36	128.15
	0.10	3.4007	15.889	17.197	35.981	51.191	54.479	88.052	89.861	103.24	103.90
60°	0.0125	3.4244	15.286	51.557	101.99	107.76	113.39	189.66	217.57	226.24	258.15
	0.025	3.4115	15.187	50.976	54.302	94.328	105.20	131.92	149.27	175.75	175.77
	0.05	3.4003	14.941	30.008	49.340	76.258	79.187	93.283	113.60	118.03	131.48
	0.10	3.3859	14.062	19.025	38.448	53.015	54.692	87.226	92.117	101.50	102.45

large for the thin plate. The mode shapes of the thick plates switch with each other when K is large. The first torsional and second bending modes switch with each other as K varies from 0° to 30° for the plate ($t/b = 0.025$), and as K varies from 30° to 60° for the plate ($t/b = 0.05, 0.10$), for instance.

Table 6 and Fig. 4 provide the results of the long cantilever plates with $a/b = 2.0$. Most of the frequency parameters are larger than those in Tables 4 and 5 and an exchange of mode shapes is the main manifestation caused by the thickness ratio and the twist angle. The bending and torsional modes appear one by one and in-plane mode shapes insert into the mode sequence with t/b increasing for the un-twisted plate, but the situation changes after the plate is subjected to twist and the bending modes in x direction occur easily. It is obvious that the mode shapes switch with each other and change their positions with t/b increasing for the twisted plates, and a torsional mode is advanced comparing with the same order of a bending mode, which means that the effect of the thickness ratio on the torsional vibration is larger than that on the bending vibration. The changes in the third bending and third torsional modes of the plate ($K = 60°$) is an example. From the changes in the mode shapes with the twist angle, it is known that the bending modes are advanced and the torsional modes are delayed with K increasing, which is more

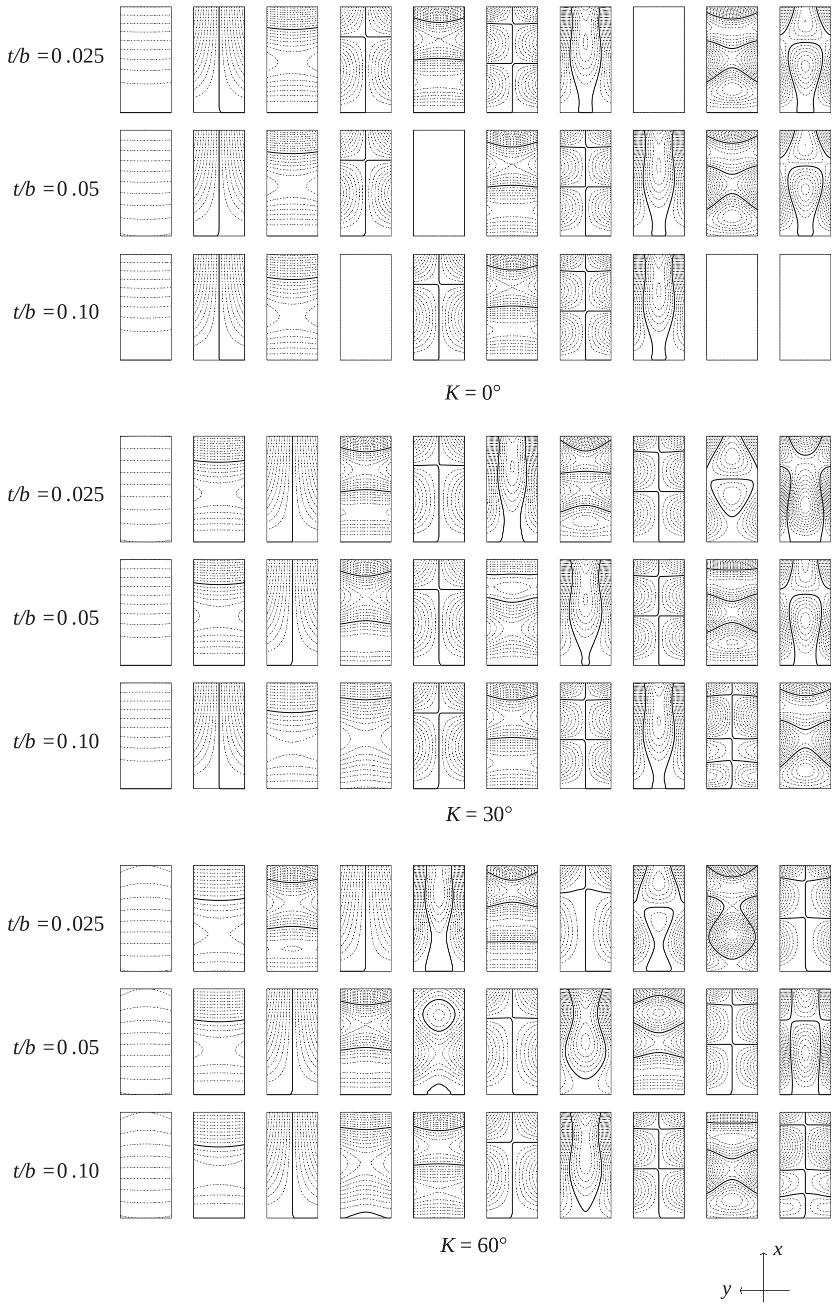

Fig. 4. Vibration mode shapes of plates ($a/b = 2.0$).

apparent for the thin plates ($t/b = 0.025$). The frequency parameters of the first third bending modes show a decrease but those of the first third torsional modes show an increase as the twist angle increases.

5. Conclusions

An equation of equilibrium for free vibration of a twisted plate is formulated by the principle of virtual work, where a strain–displacement relationship of a twisted plate is derived by Green strain tensor on general shell theory and the first order shear deformation theory. The governing equation is obtained by the Rayleigh–Ritz method with three linear and two angular displacement functions defined by sets of orthonormal polynomials which are generated by the Gram–Schmidt process. A cantilever twisted plate is chosen as an example of numerical analysis. Comparing with the previous results by the methods based on the classical thin shell theory and the Mindlin plate theory, a very good agreement reveals the accuracy and practicability of the present method, and it is also demonstrated that the present method is applicable to thin and Mindlin twisted plates. The frequency parameters and mode shapes of cantilever plates with various twist angles, aspect ratios and thickness ratios are achieved by the present method.

It is known that an increase in the thickness or the transverse shear deformation makes frequency parameters of bending and torsional vibrations to decrease for the plates, which there are no such effects on mode shapes of the un-twisted plates. There are different effects related to twist angles and types of modes for the twisted plates. The greater the aspect ratio is, the greater the frequency parameters are, but the variations of the lower frequency parameters are small and those of the higher ones are large. However, the torsional frequency parameters increase and the bending ones decrease with an increase in the twist angle.

Acknowledgements

The manuscript of this paper was completed when the first author (X. X. HU) was at Nagasaki University, Japan, as a foreign researcher. The support provided by the Japan Society for the Promotion of Science is greatly appreciated.

Appendix A

$\mathscr{G}^{(1)}$ and $\mathscr{G}^{(2)}$ are 10×9 and 10×6 dimensional matrices, and their non-zero elements are defined as

$$\mathscr{G}^{(1)}_{1,1} = \sqrt{g}, \quad \mathscr{G}^{(1)}_{1,6} = \frac{K^2 Y}{\sqrt{g}}, \quad \mathscr{G}^{(1)}_{2,2} = \frac{a}{b} K, \quad \mathscr{G}^{(1)}_{2,3} = \frac{b}{a} \frac{K^3 Y}{\sqrt{g}}, \quad \mathscr{G}^{(1)}_{2,9} = -\frac{K^2}{g\sqrt{g}}, \quad \mathscr{G}^{(1)}_{3,5} = \frac{a}{b} \sqrt{g},$$

$$\mathscr{G}^{(1)}_{4,3} = -\frac{K^3 Y}{g}, \mathscr{G}^{(1)}_{4,4} = \frac{K}{g}, \quad \mathscr{G}^{(1)}_{4,9} = -\frac{K^2}{g\sqrt{g}}, \quad \mathscr{G}^{(1)}_{5,2} = \frac{a}{b} g, \quad \mathscr{G}^{(1)}_{5,3} = -K^2 Y\left(\frac{b}{a} - 1\right),$$

$$\mathscr{G}^{(1)}_{5,4} = 1.0, \quad \mathscr{G}^{(1)}_{5,9} = -\frac{2K}{\sqrt{g}}, \mathscr{G}^{(1)}_{6,1} = \frac{K}{\sqrt{g}}, \quad \mathscr{G}^{(1)}_{6,5} = \frac{a}{b} \frac{K}{\sqrt{g}}, \quad \mathscr{G}^{(1)}_{6,6} = \frac{K^3 Y}{g\sqrt{g}}, \quad \mathscr{G}^{(1)}_{7,3} = K, \quad \mathscr{G}^{(1)}_{7,8} = \frac{a}{b}\sqrt{g},$$

$$\mathscr{G}^{(1)}_{8,6} = \frac{K^2}{g\sqrt{g}}, \ \mathscr{G}^{(1)}_{8,7} = \frac{K}{g}, \quad \mathscr{G}^{(1)}_{9,6} = \frac{K}{\sqrt{g}}, \quad \mathscr{G}^{(1)}_{9,7} = 1.0, \quad \mathscr{G}^{(1)}_{10,3} = \frac{K^2}{g}, \quad \mathscr{G}^{(1)}_{10,8} = \frac{a}{b}\frac{K}{\sqrt{g}},$$

$$\mathscr{G}^{(2)}_{7,6} = \sqrt{g}, \quad \mathscr{G}^{(2)}_{8,3} = K, \quad \mathscr{G}^{(2)}_{9,3} = g, \ \mathscr{G}^{(2)}_{10,6} = \frac{K}{\sqrt{g}}, \tag{A.1}$$

and

$$\boldsymbol{\mathscr{G}}^{(2)}_{i,j} = \boldsymbol{\mathscr{G}}^{(1)}_{i,j} \quad (i = 1\text{–}6, \ j = 1\text{–}6). \tag{A.2}$$

References

[1] A.W. Leissa, Vibration of Plates (NASA SP-160). Office of Technology Utilization, NASA, Washington DC, 1973.
[2] A.W. Leissa, Recent studies in plate vibration: 1981–1985 part I, classical theory, *Shock and Vibration Digest* 19 (2) (1987) 11–18.
[3] A.W. Leissa, Recent studies in plate vibration: 1981–1985 part II, complicating effects, *Shock and Vibration Digest* 19 (3) (1987) 10–24.
[4] M. Sathyamoorthy, Nonlinear vibration analysis of plates: a review and survey of current developments, *Applied Mechanics Reviews* 40 (11) (1987) 1553–1561.
[5] K.M. Liew, Y. Xiang, S. Kitipornchai, Research on thick plate vibration: a literature survey, *Journal of Sound and Vibration* 180 (1) (1995) 163–176.
[6] R.B. Bhat, Natural frequencies of rectangular plates using characteristic orthogonal polynomials in Rayleigh–Ritz method, *Journal of Sound and Vibration* 102 (4) (1985) 492–499.
[7] B. Singh, S. Chakraverty, On the use of orthogonal polynomials in the Rayleigh–Ritz method for the study of transverse vibration of elliptic plates, *Computers and Structures* 43 (3) (1992) 439–443.
[8] B. Singh, S. Chakraverty, Flexural vibration of skew plates using boundary characteristic orthogonal polynomials in two variables, *Journal of Sound and Vibration* 173 (2) (1994) 157–178.
[9] S.M. Dickinson, A. Di-Blasio, On the use of orthogonal polynomials in the Rayleigh–Ritz method for the study of flexural vibration and buckling of isotropic and orthotropic rectangular plates, *Journal of Sound and Vibration* 108 (1) (1986) 51–62.
[10] K.M. Liew, K.Y. Lam, Application of two-dimensional orthogonal plate function to flexural vibration of skew plates, *Journal of Sound and Vibration* 139 (2) (1990) 241–252.
[11] K.M. Liew, C.M. Wang, pb-2 Rayleigh–Ritz method for general plate analysis, *Engineering Structures* 15 (1993) 55–60.
[12] K.M. Liew, K.C. Hung, K.M. Lim, Vibration of Mindlin plate using boundary characteristic orthogonal polynomials, *Journal of Sound and Vibration* 182 (1) (1995) 77–90.
[13] S. Chakraverty, R.B. Bhat, I. Stiharu, Recent research on vibration of structures using boundary characteristic orthogonal polynomials in the Rayleigh–Ritz method, *Shock and Vibration Digest* 31 (3) (1999) 187–194.
[14] J.C. Macbain, Vibratory behavior of twisted cantilevered plates, *Journal of Aircraft* 12 (4) (1975) 343–349.
[15] R. Kielb, A.W. Leissa, J.C. Macbain, Vibrations of twisted cantilevered plates—A comparison of theoretical results, *International Journal for Numerical Methods in Engineering* 21 (8) (1985) 1365–1380.
[16] T. Tsuiji, T. Sueoka, Free vibration of pre-twisted plates (fundamental theory), *Transaction of the Japan Society of Mechanical Engineering* 52(C) (484) (1986) 3042–3046 (in Japanese).
[17] T. Tsuiji, K. Kaneko, T. Sueoka, Free vibration of pre-twisted plates (numerical results by Rayleigh–Ritz method), *Transaction of the Japan Society of Mechanical Engineering* 53(C) (487) (1987) 605–611 (in Japanese).